DESCRIPTION OF A METHOD FOR MEASURING THE DIFFUSION COEFFICIENT OF THIN FILMS TO ^{222}Rn USING A TOTAL ALPHA DETECTOR

Ronald B. Mosley
U.S. EPA, National Risk Management Research Laboratory, Air Pollution Prevention and Control Division
Research Triangle Park, NC

ABSTRACT

The present paper describes a method for using a total alpha detector to measure the diffusion coefficient of a thin film by monitoring the accumulation of radon that penetrates the film. It will be demonstrated that a virtual steady state condition exists in the thin film during the early stages of accumulation that allows reliable measurements of the diffusion coefficient without having to wait for the final condition of equilibrium or having to analyze the complex transient solutions. In some cases, the final condition of equilibrium would require the measurement to last three or more weeks rather than three days.

INTRODUCTION

While it has been accepted for some time that exposure to indoor radon constitutes a potentially serious health threat, it has become increasingly apparent that the construction industry prefers a passive mitigation method of preventing entry of radon into the indoor environments. One such method, applicable to new construction, consists of installing passive barriers such as a thin membrane to prevent ingress of radon gas into the indoor environment. Such a barrier would need to control both advective and diffusive transport of radon. Use of a membrane as a barrier has the advantage over other approaches of serving multiple purposes. Membranes are currently specified in many localities for moisture control. In order to investigate the applicability of new materials for use as membranes, a simple and convenient method of measuring the diffusivity of thin films is needed. The present paper discusses a laboratory method for measuring the ^{222}Rn diffusion coefficient using a total alpha detector. The apparatus is described by Perry and Snoddy (1996) and will not be discussed in detail here. A number of studies: Nielson, K.K. at el. (1981), Nielson, K.K., Rich, D.C., and Rogers, V.C. (1982), Jha, G., Raghavayya, M, and Padmanabhan, H. (1982), Rogers, V.C., and Nielson, K.K. (1984), Hafez, A. And Somogyi, G. (1986), and Nielson, K.K., Holt, R.B., and Rogers, V.C. (1996) have addressed the measurement of ^{222}Rn diffusion through barriers including films, soils, and concrete. These methods used either the steady state solution for diffusion or a very complex transient solution. The present paper proposes a simpler mathematical solution to use which describes a virtual steady state that exist when the concentration at one interface of the film increases very slowly with time.

This paper has been reviewed in accordance with the U.S. Environmental Protection Agency's peer and administrative review policies and approved for presentation and publication.

MATHEMATICAL MODEL

In order to test a film's resistance to radon transport, the film will be placed between a chamber containing a source of radon and a chamber that accumulates the radon transported through the film. The tests will be performed under ambient conditions. It is assumed that no advective transport through the film occurs. A schematic of this arrangement is illustrated in figure 1. Region 1 represents the radon source in which the radon concentration is assumed to remain constant during the measurements. Region 2 corresponds to the film to be tested. The transport equation that applies in Region 2 is given by

$$\frac{\partial C}{\partial t} = D\frac{\partial^2 C}{\partial x^2} - \lambda_{Rn} C \qquad (1)$$

where C is the radon concentration (Atoms m^{-3}) in the film, t is the time (s), D is the diffusion coefficient ($m^2 s^{-1}$) in the film , x is the position (m) within the film, and λ_{Rn} is the decay constant (s^{-1}) for ^{222}Rn. In general, the concentration [C(x,t)] within the film is a function of both position and time. The non-steady solution of Equation 1 can be expressed as an infinite sum of position dependent trigonometric functions multiplied by an exponentially decreasing time function (Crank, 1994). Colle_ et al (1981) and Crank (1994) have shown that the relaxation time, τ_r, associated with the approach to steady state is given approximately by $\tau_r = (\lambda_{Rn} + \pi^2 D d^{-2})^{-1}$, where d is the thickness (m) of the film. When the film is 1.27×10^{-4} m (5 mils) thick, the relaxation time is about 0.3 minutes for a diffusion coefficient of 10^{-10} $m^2 s^{-1}$ and about 4 hours for a diffusion coefficient of 10^{-13} m^2 s^{-1}. This three order-of-magnitude range in diffusion coefficient is believed to include most of the commonly used construction films. After a time corresponding to several multiples of τ_r, the film can be assumed to be in a steady state provided the concentrations at the boundaries remain constant. In fact we define the condition in the film in which the concentrations at the boundaries do not change significantly during times that are long compared to the relaxation time as a condition of virtual steady state. During a virtual steady state, the flux is nearly constant during times comparable with τ_r. Approximate solutions to equation 1 corresponding to the condition of a virtual steady state will be used to avoid the very complex analysis associated with non-steady state solutions.

Region 3 is a closed volume in which ^{222}Rn accumulates. Consequently, the concentration at the surface of the film, C_d, will slowly increase with time to match the increasing concentration in region 3, $C_a(t)$. The condition of virtual steady state in the film will continue to apply so long as the fractional change in $C_a(t)$ is small during time intervals comparable to the relaxation time. The appropriate boundary conditions for the virtual steady state are $C(0) = C_s$, the concentration in region 1, and $C(d) = C_a(t)$.

The virtual steady state condition is determined by letting the time derivative of C go to zero. Equation 1 then becomes

$$D\frac{d^2 C}{dx^2} - \lambda_{Rn} C = 0 \qquad (2)$$

with boundary conditions: $C(0) = C_s$ and $C(d) = C_d = C_a$, where C_a is the concentration in region 3. We assume that region 3 remains well mixed. The solution to equation 2 is

$$C(x) = \frac{C_s \operatorname{Sinh}\sqrt{\frac{\lambda_{Rn}}{D}}(d-x) + C_d \operatorname{Sinh}\sqrt{\frac{\lambda_{Rn}}{D}}x}{\operatorname{Sinh}\sqrt{\frac{\lambda_{Rn}}{D}}d} \qquad (3)$$

Also note that

$$\frac{dC}{dx}_{-x=d} = -\sqrt{\frac{\lambda_{Rn}}{D}}\left[\frac{C_s - C_d \ \mathrm{Cosh}\sqrt{\frac{\lambda_{Rn}}{D}}\, d}{\mathrm{Sinh}\sqrt{\frac{\lambda_{Rn}}{D}}\, d}\right] \tag{4}$$

Region 3 is an accumulation chamber. The radon concentration in this chamber will be measured as a function of time. Measuring the rate of increase of radon in Region 3 gives a direct measurement of the flux from the surface of the film. This flux is easily computed when transport through the film remains in a virtual steady state condition. Mass balance in region 3 requires that

$$\frac{dC_a}{dt} = \frac{\beta(t)}{V_a} - \lambda_{Rn} C_a \tag{5}$$

where $C_a(t)$ is the ^{222}Rn concentration (atoms m^{-3}) in region 3, $\beta(t)$ is the rate of transport (atoms s^{-1}) of ^{222}Rn atoms through the film, and V_a is the volume (m^3) of region 3. In a steady state $\beta(t)$ is given by

$$\beta(t) = -D\frac{dC}{dx}_{-x=d} A = \beta_0\left(1 - \frac{C_a(t)}{C_s}\ \mathrm{Cosh}\sqrt{\lambda_{Rn} overD}\, d\right) \tag{6}$$

where A is the cross sectional area (m^2) of the film and

$$\beta_0 = \frac{AD C_s \sqrt{\frac{\lambda_{Rn}}{D}}}{\mathrm{Sinh}\sqrt{\frac{\lambda_{Rn}}{D}}\, d} \tag{7}$$

Equation 5 then becomes

$$\frac{dC_a}{dt} + (\lambda_{Rn} + \lambda_\beta)\, C_a = \frac{\beta_0}{V_a} \tag{8}$$

where

$$\lambda_\beta = \frac{\beta_0 \ \mathrm{Cosh}\sqrt{\frac{\lambda_{Rn}}{D}}\, d}{V_a C_s} \tag{9}$$

The solution of equation 8 is

$$C_a(t) = \frac{\beta_0}{V_a(\lambda_{Rn} + \lambda_\beta)} \{1 - \exp(-[\lambda_{Rn} + \lambda_\beta]t)\} \tag{10}$$

After substituting equation 10 into 6 and rearranging, we may write

$$\beta(t) = \beta_\infty + (\beta_0 - \beta_\infty) \exp(-[\lambda_{Rn} + \lambda_\beta]t) \tag{11}$$

where

$$\beta_\infty = \beta_0 \left(1 - \frac{\beta_0 \mathrm{Cosh}\sqrt{\frac{\lambda_{Rn}}{D}}\, d}{C_s V_a(\lambda_{Rn} + \lambda_\beta)}\right. \tag{12}$$

Equation 10 expresses the ^{222}Rn concentration in region 3, while equation 11 gives the rate of transport of atoms through the film. If ^{222}Rn concentration were being measured directly in this experiment, these equations would be sufficient to yield a value of diffusion coefficient. However, in the current set of measurements, the total alpha activity was measured. These measured values contain contributions from ^{222}Rn, ^{218}Po, and ^{214}Po. Since the third alpha particle is emitted during the fourth decay step following radon, it is necessary to solve all the decay rate equations (Bateman equations) in sequence. These equations are given by

^{222}Rn:

$$\frac{dN_{Rn}}{dt} = - \lambda_{Rn} N_{Rn} + \beta(t) \tag{13}$$

^{218}Po:

$$\frac{dN_A}{dt} = - \lambda_A N_A + \lambda_{Rn} N_{Rn} \tag{14}$$

^{214}Pb:

$$\frac{dN_B}{dt} = -\lambda_B N_B + \lambda_A N_A \tag{15}$$

^{214}Bi:

$$\frac{dN_C}{dt} = -\lambda_C N_C + \lambda_B N_B \tag{16}$$

where N_{Rn} is the number of ^{222}Rn atoms present, λ_{Rn} (2.1×10^{-6} s^{-1}) is their decay constant, N_A is the number of ^{218}Po atoms, λ_A (3.80×10^{-3} s^{-1}) is their decay constant, N_B is the number of ^{214}Pb atoms, λ_B (4.32×10^{-4} s^{-1}) is their decay constant, N_C is the number of ^{214}Bi atoms, and λ_C (5.87×10^{-4} s^{-1}) is their decay constant. Because ^{214}Po which produces the third alpha particle has a half-life of only 1.6×10^{-4} s, it is assumed to occur simultaneously with ^{214}Bi. Consequently, only four rate equations will be solved. Note that these equations must be solved sequentially and the resulting solutions substituted into the next equation. Equations 13 through 16 differ from the traditional Bateman equations in that the ^{222}Rn concentration is increasing with time.

Decays that give rise to alpha activity are represented by

^{222}Rn:

$$\lambda_{Rn} N_{Rn} \approx \frac{\lambda_{Rn} \beta_0}{\lambda_{Rn} + \lambda_\beta} \{1 - \exp(-[\lambda_{Rn} + \lambda_\beta] t)\} \tag{17}$$

^{218}Po:

$$\lambda_A N_A = \frac{\lambda_{Rn} \beta_0}{\lambda_{Rn} + \lambda_\beta} \{1 + (\frac{\lambda_{Rn} + \lambda_\beta}{\lambda_A - \lambda_{Rn} - \lambda_\beta}) \exp(-\lambda_A t) - (\frac{\lambda_A}{\lambda_A - \lambda_{Rn} - \lambda_\beta}) \exp(-[\lambda_{Rn} + \lambda_\beta] t)\} \tag{18}$$

$$\lambda_C N_C \approx \frac{\lambda_{Rn}\beta_0}{\lambda_{Rn}+\lambda_\beta}\Big\{1 + \frac{\lambda_B\lambda_C(\lambda_{Rn}+\lambda_\beta)}{(\lambda_A-\lambda_{Rn}-\lambda_\beta)(\lambda_A-\lambda_B)(\lambda_A-\lambda_C)}\exp(-\lambda_A t)$$
$$+ \Big[\frac{\lambda_A\lambda_B\lambda_C}{(\lambda_A-\lambda_{Rn}-\lambda_\beta)(\lambda_B-\lambda_{Rn}-\lambda_\beta)(\lambda_C-\lambda_B)} + \frac{\lambda_B\lambda_C(\lambda_{Rn}+\lambda_\beta)}{(\lambda_A-\lambda_{Rn}-\lambda_\beta)(\lambda_A-\lambda_B)(\lambda_C-\lambda_B)}$$
$$- \frac{\lambda_C}{\lambda_C-\lambda_B}\Big]\exp(-\lambda_B t) - \Big[1 + \frac{\lambda_A\lambda_B\lambda_C}{(\lambda_A-\lambda_{Rn}-\lambda_\beta)(\lambda_B-\lambda_{Rn}-\lambda_\beta)(\lambda_C-\lambda_B)}$$
$$+ \frac{\lambda_B\lambda_C(\lambda_{Rn}+\lambda_\beta)}{(\lambda_A-\lambda_{Rn}-\lambda_\beta)(\lambda_A-\lambda_B)(\lambda_C-\lambda_B)} + \frac{\lambda_B\lambda_C(\lambda_{Rn}+\lambda_\beta)}{(\lambda_A-\lambda_{Rn}-\lambda_\beta)(\lambda_A-\lambda_B)(\lambda_A-\lambda_C)}$$
$$- \frac{\lambda_C}{(\lambda_C-\lambda_B)} - \frac{\lambda_A\lambda_B\lambda_C}{(\lambda_A-\lambda_{Rn}-\lambda_\beta)(\lambda_B-\lambda_{Rn}-\lambda_\beta)(\lambda_C-\lambda_{Rn}-\lambda_\beta)}\Big]\exp(-\lambda_C t)$$
$$- \frac{\lambda_A\lambda_B\lambda_C}{(\lambda_A-\lambda_{Rn}-\lambda_\beta)(\lambda_B-\lambda_{Rn}-\lambda_\beta)(\lambda_C-\lambda_{Rn}-\lambda_\beta)}\exp(-[\lambda_{Rn}+\lambda_\beta]t)\Big\} \quad (19)$$

As explained above, the third alpha particle is actually emitted by ^{214}Po. However, it occurs so shortly after the ^{214}Bi decay that we consider them to be simultaneous.

The total measured activity , MA, (decays s^{-1}) is given by

$$MA = \lambda_{Rn}\, N_{Rn}\, E_{Rn} + \lambda_A\, N_A\, E_A + \lambda_C\, N_C\, E_{C'} \quad (20)$$

where E_{Rn} is the efficiency of the detector for the first alpha particle, E_A is the efficiency for the second alpha particle, and $E_{C'}$ is the efficiency for the third alpha particle. Keeping only the dominant terms in equations 17 - 19, equation 20 becomes

$$MA = \frac{\lambda_{Rn}\beta_0}{\lambda_{Rn}+\lambda_\beta}(E_{Rn}+E_A+E_{C'})\Big\{1-\exp(-[\lambda_{Rn}+\lambda_\beta]t)\Big\}$$
$$+\frac{E_A}{\lambda_A}\exp(-\lambda_A t) + \frac{\lambda_B\lambda_C E_{C'}}{\lambda_A(\lambda_C-\lambda_B)}\Big[\frac{\exp(-\lambda_B t)}{(\lambda_A-\lambda_B)} - \frac{\exp(-\lambda_C t)}{(\lambda_A-\lambda_C)}\Big] \quad (21)$$

When $\lambda^{-1}_A \ll t$, the last three terms in equation 21 can be neglected, so that Equation 22 is just a convenient mathematical form in which the constants α and γ are parameters to be chosen to yield the best fit to the data. By

comparing equations 21 and 22, it follows that

$$MA = \alpha[1-\exp(-\gamma t)] \tag{22}$$

Equation 22 is just a convenient mathematical form in which the constants a and y are parameters to be chosen to yield the best fit to the data. By comparing equations 21 and 22, it follows that

$$D = (\gamma - \lambda_{Rn})\, dL \frac{\tanh\sqrt{\frac{\lambda_{Rn}}{D}}d}{\sqrt{\frac{\lambda_{Rn}}{D}}d} \tag{23}$$

Equation 23, which contains one of the fitting parameters, γ, is transcendental. It must be solved numerically or iterated to obtain the diffusion coefficient, D. However, when $(\lambda_{Rn} / D)^{1/2}\, d << 1$, the last equation becomes

$$D = (\gamma - \lambda_{Rn})dL \tag{24}$$

Equation 23 or 24 provides a measured value of the diffusion coefficient whose accuracy depends upon the degree to which the measured activity fits the expression in equation 22. For a highly accurate fit, one needs to extend the measurements until the curve begins to approach its maximum value. For films with low values of diffusion coefficient, these measurements can require many days or even a few weeks. Since shorter measurement times would be convenient, we choose to analyze the early stages of the measurements. In the range that $\lambda^{-1}_{A} << t << (\lambda_{Rn} + \lambda_{\beta})^{-1}$, equation 21 reduces to

$$MA \approx \lambda_{Rn}\beta_0(E_{Rn} + E_A + E_{C'})t \tag{25}$$

which is linear with time. The diffusion coefficient is related to the slope, S_R, of the linear portion of the curve by

$$D = \frac{S_R dL}{\lambda_{Rn} C_s V_a (E_{Rn} + E_A + E_{C'})} \frac{\sinh\sqrt{\frac{\lambda_{Rn}}{D}}\, d}{\sqrt{\frac{\lambda_{Rn}}{D}}\, d} \tag{26}$$

The slope, S_R, can be determined by a regression fit to the linear portion of the curve. Equation 26 is transcendental and cannot be solved explicitly for D. Simple numerical methods will provide a solution of this equation. However,

when $(\lambda_{Rn} / D)^{1/2} d << 1$, equation 26 reduces to

$$D = \frac{S_R d L}{\lambda_{Rn} C_s V_a (E_{Rn} + E_A + E_{C'})} \tag{27}$$

This approximation is typically valid for 1.27×10^{-4} m (5 mil) thick films whose diffusion coefficients are greater than 1.0×10^{-12} m^2 s^{-1}. Note that both equations 26 and 27 contain the total efficiency of the alpha detector. In general this quantity will be determined by an independent calibration and depends on the geometry of both the detector and the chamber. For the present set of measurements, the total efficiency can be determined from a series of longer measurements using equation 22. In terms of the parameters used to fit equation 22, the efficiency becomes

$$E_{Rn} + E_A + E_{C'} = \frac{\alpha\gamma}{\lambda_{Rn} C_s V_a (\gamma - \lambda_{Rn})} \frac{\cosh\sqrt{\frac{\lambda_{Rn}}{D}}\, d}{\sqrt{\frac{\lambda_{Rn}}{D}}\, d} \tag{28}$$

When $(\lambda_{Rn} / D)^{1/2} << 1$, the efficiency becomes

$$E_{Rn} + E_A + E_{C'} = \frac{\alpha\gamma}{\lambda_{Rn} C_s V_a (\gamma - \lambda_{Rn})} \tag{29}$$

Once an average value of efficiency has been established using equation 28 or 29, then shorter runs can be used to compute the diffusion coefficient using either equation 26 or 27.

DATA ANALYSIS

Measurements have been performed on a large number of films. Several of these measurements are considered preliminary and are not reported here. In an effort to evaluate the feasibility of performing short term tests to measure diffusion coefficients of thin films, we will analyze duplicate measurements on two materials, polyethylene and natural latex rubber. Figures 2 and 3 show measurements on two polyethylene films 1.524×10^{-4} m (6 mil) thick. Background counts and the initial data prior to the virtual steady state have been subtracted. More than 8,000 one-minute counts are represented by tiny squares in the figures. The line through the data points represents a least-square fit to equation 22, utilizing the methods of Levenberg and Marquardt to determine the fitting parameters. The parameters yielding the best fit to equation 22 are shown in the figures. For convenience the time is plotted in units of hours, however, the equations illustrated in the figures use seconds. The coefficients of

determination for these fits are also shown. As is illustrated by the values of R^2 , the degree of agreement with the mathematical equation is excellent. Less than 0.1% of the variation is unexplained.

Figure 4 shows the early data in Figure 2. The tiny squares represent measurements while the line represents a linear regression analysis. The regression slope and the coefficient of determination for the fit are given in the figure. Once again the degree of fit is very good. The regression slope can be used in equation 26 or 27 to calculate the diffusion coefficient. For present materials, equation 27 yields a reasonable estimate of the diffusion coefficient. An improved value is obtained when the initial estimate from equation 27 is used to evaluate the right hand side of equation 26. The new value of D obtained in equation 26 can be used iteratively to compute an improved solution of equation 26. In the present case, convergence is adequate after only two iterations. The linear segment corresponding to the initial data in Figure 3 is shown in Figure 5. Once again, linear regression analysis yields the slope and the coefficient of determination. Equation 26 yields the diffusion coefficient. The diffusion coefficients for all four figures are given in Table 1. It can also be seen from Table 1 that the values of diffusion coefficient computed from the initial data differ by only 9% and 12% from the values computed from the full curves.

Figures 6 and 7 show the accumulation curves for total alpha activity when ^{222}Rn diffuses through two similar films of natural latex rubber 1.225×10^{-4} m thick. The curve through the data represents a least-square fit. The fit parameters and the coefficient of determination are shown. Figure 8 illustrates the early portion of the data in Figure 6. Note that the curve is quite linear. The regression slope and coefficient of determination are shown on the figure. Figure 9 illustrates the early data in Figure 7. The diffusion coefficients computed from these fits are given in Table 1. Note that the agreement between the diffusion coefficients computed by the two methods is not as good for the latex films. This may be due, in part, to the fact that much less data is used in the calculation for latex. The linear portion of the curve exist for a much shorter time. In this case, however, it is quite practical to extend the curve sufficiently to obtain a reliable fit to equation 22.

CONCLUSIONS

While equation 23 works quite well for determining the diffusion coefficient of thin films, it may require very long times to sufficiently complete the shape of the curve to yield good accuracy. It has been demonstrated that shorter measurements along with the use equation 26 yield an adequate determination of the diffusion coefficient in some cases. This method appears to work for diffusion coefficients in the range 10^{-10} m^2 s^{-1} to 10^{-12} $m^2 s^{-1}$. It is estimated that the method should be applicable for values that are two-orders-of-magnitude lower.

These measured diffusion coefficients appear to be largely consistent with values reported for similar materials. For instance, the average value for polyethylene, 8.81×10^{-12} m^2 s^{-1} , differs by only 12% from the value, 7.8×10^{-12} m^2 s^{-1}, reported by Hafex and Somogyi (1986). The average value for latex, 1.43 10^{-10} m^2 s^{-1}, differs by 127% form the value, 6.36×10^{-10} m^2 s^{-1}, reported by Jha, Raghavayya, and Padmanabhan (1982). While these results are relatively consistent, little is known about just how similar the materials really were.

REFERENCES

Colle', R., Rubin, R.J., Knab, L.I., and Hutchinson, J.M.R. Radon transport through and exhalation from building materials: A review and assessment. NBS Technical Note 1139, Sept. 1981.
Crank, J. The mathematics of diffusion. Clarendon Press, Oxford, 1994.

Hafez, A. And Somogyi, G. Determination of Radon and Thoron permeability through some plastics by track technique. Nuclear Tracks, Vol 12, Nos 1-6, pp 697-700, 1986.

Jha, G., Raghavayya, M., and Padmanabhan, H. Radon permeability of some membranes. Health Physics, Vol 42. No 5, pp 723-725, 1982.

Nielson, K.K., Rogers, V.C., Rich, D.C., Nederhand, P.A.., Sandquist, G.M., and Jensen, C.M. Laboratory measurements of radon diffusion through multilayered cover systems for uranium tailings. Department of Energy Report UMT/0206, December, 1981.

Nielson, K.K., Rich, D.C., and Rogers, V.C. Comparison of radon diffusion coefficients measured by transient diffusion and steady-state laboratory methods. Report to U.S. Nuclear Regulatory Commission, Washington, D.C., NUREG/CR-2875. 1982.

Nielson, K.K., Holt, R.B., and Rogers, V.C. Residential radon resistant construction features selection system. EPA-600/R-96-005, February, 1996.

Perry, R. and Snoddy, R. A method for testing the diffusion coefficient of polymer films. Proceedings: The 1996 International Radon Conference, Haines City, FL, Sept. 29 - Oct. 2, 1996.

Rogers, V.C., and Nielson, K.K. Radon attenuation handbook for uranium mill tailings cover design. U.S. Nuclear Regulatory Commission, Washington, D.C., NUREG/CR-3533, 1984.

Table 1. Comparison of Diffusion Results

Film	$\lambda_{Rn}C_s$ (Bq)	d (m)	E	D^{*}_{non} ($m^2 s^{-1}$)	D^{**}_{lin} ($m^2 s^{-1}$)	% diff
poly 1	2.80×10^{6}	1.524×10^{-4}	0.742	7.79×10^{-12}	6.87×10^{-12}	12
poly 2	2.95×10^{6}	1.524×10^{-4}	0.651	9.83×10^{-12}	8.91×10^{-12}	9
latex 1	2.90×10^{6}	1.225×10^{-4}	0.611	1.55×10^{-10}	1.10×10^{-10}	29
latex 2	2.93×10^{6}	1.225×10^{-4}	0.680	1.31×10^{-10}	9.37×10^{-11}	28

* D_{non} = Diffusion coefficient computed from nonlinear curve
** D_{lin} = Diffusion coefficient computed from linear curve

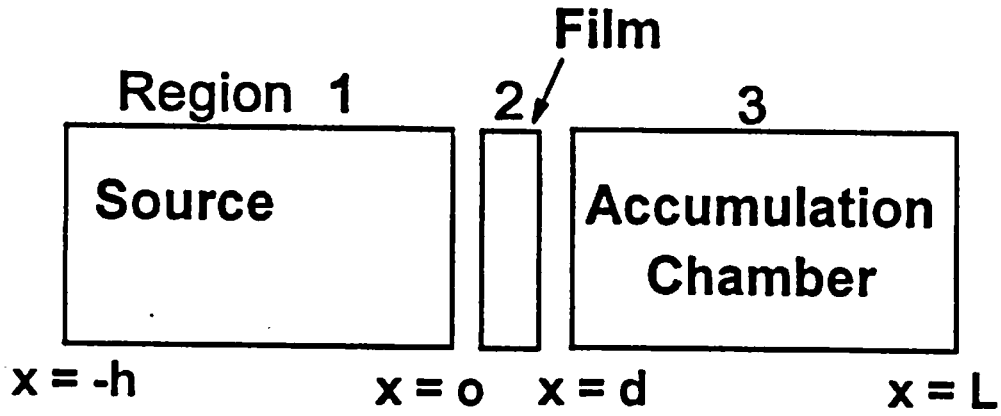

Figure 1. Schematic of the measurement system

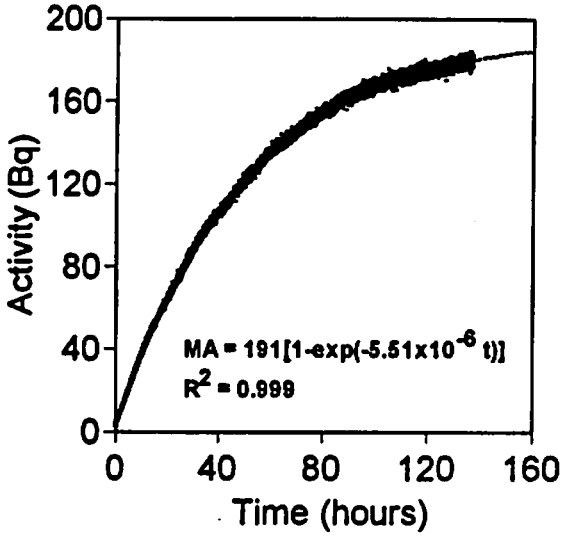

Figure 2. Accumulated activity for Poly 1

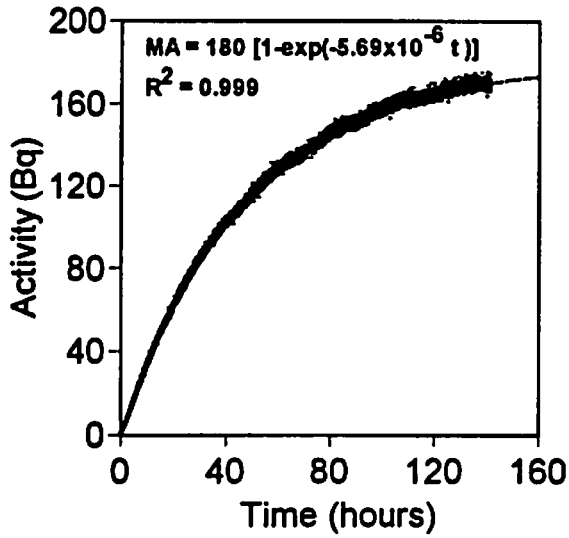

Figure 3. Accumulated activity for poly 2 film

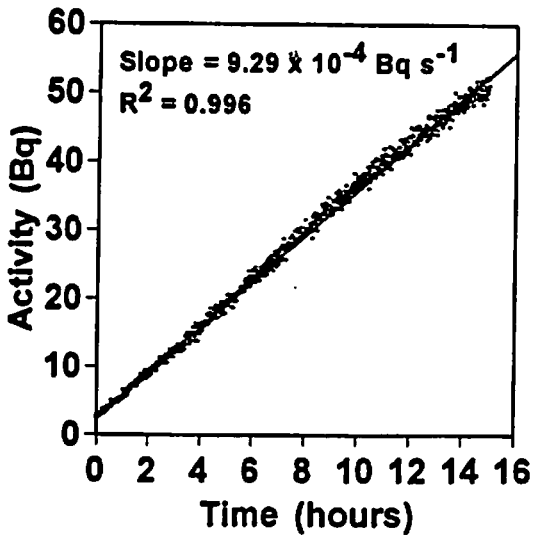

Figure 4. Linear portion of poly 1 activity curve

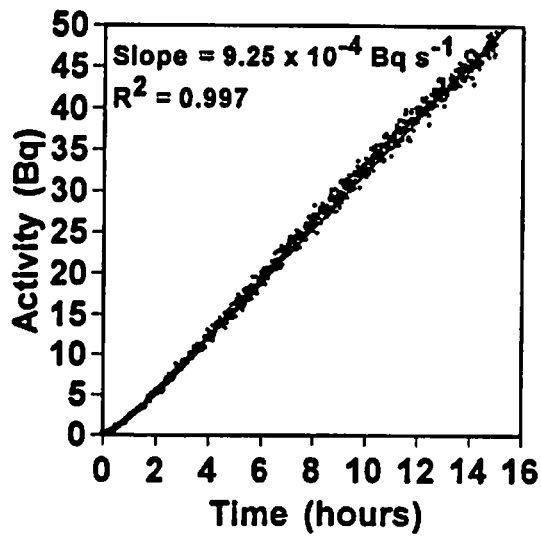

Figure 5. Linear portion of poly 2 activity curve

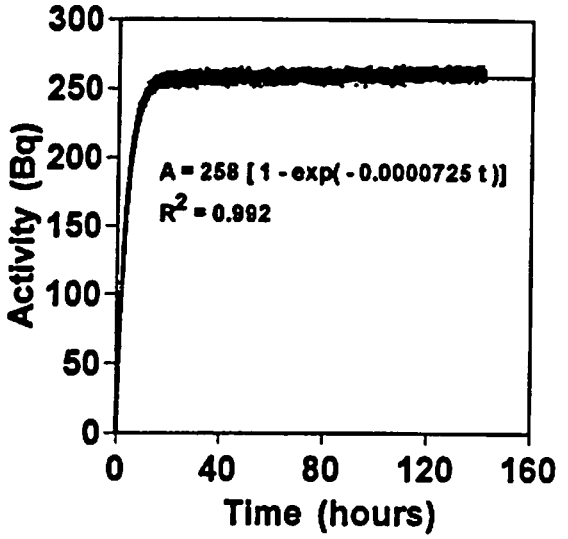

Figure 6. Accumulated activity for latex 1 film

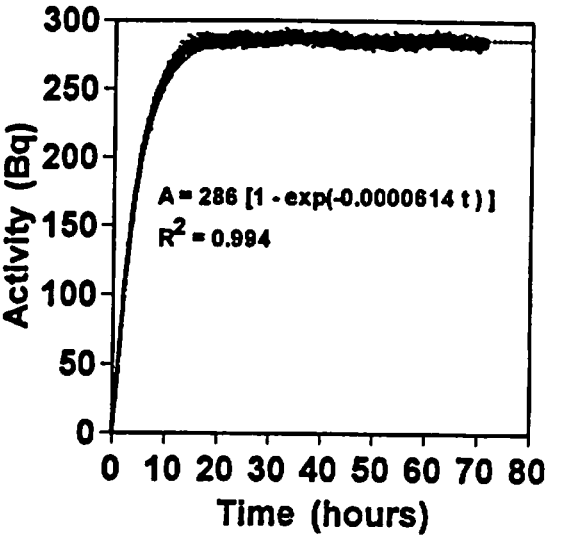

Figure 7. Accumulated activity for latex 2 film

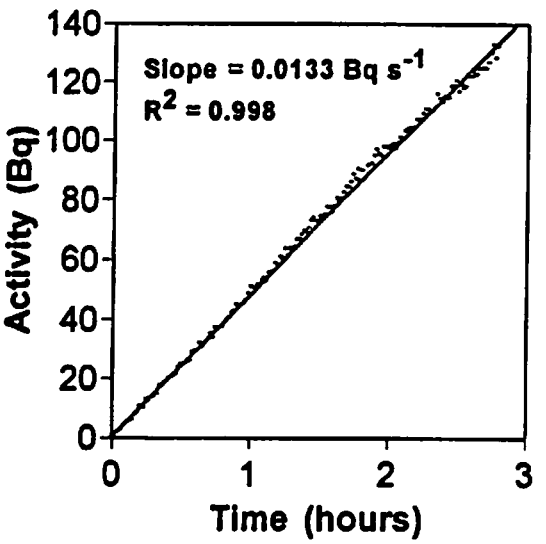

Figure 8. Linear portion of latex 1 activity curve

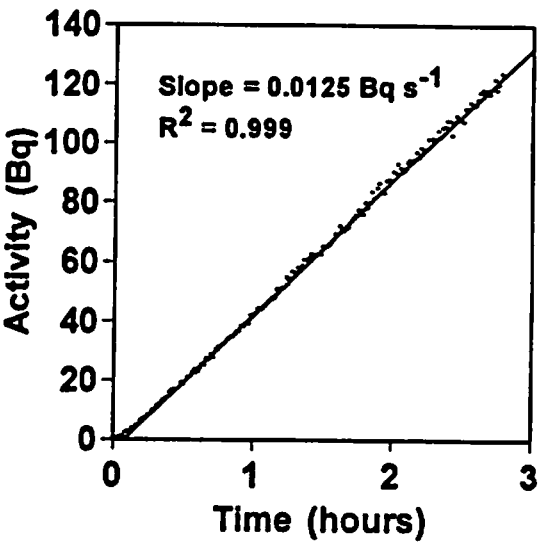

Figure 9. Linear portion of latex 2 activity curve